iScience, Volume *27*

Supplemental information

Spatiotemporal dynamics exhibited by horizontal basal cells reveal a pro-neurogenic pathway during injury-induced olfactory epithelium regeneration

Jonathan D. Louie, Camila M. Barrios-Camacho, Benjamin H. Bromberg, Constantin A. Hintschich, and James E. Schwob

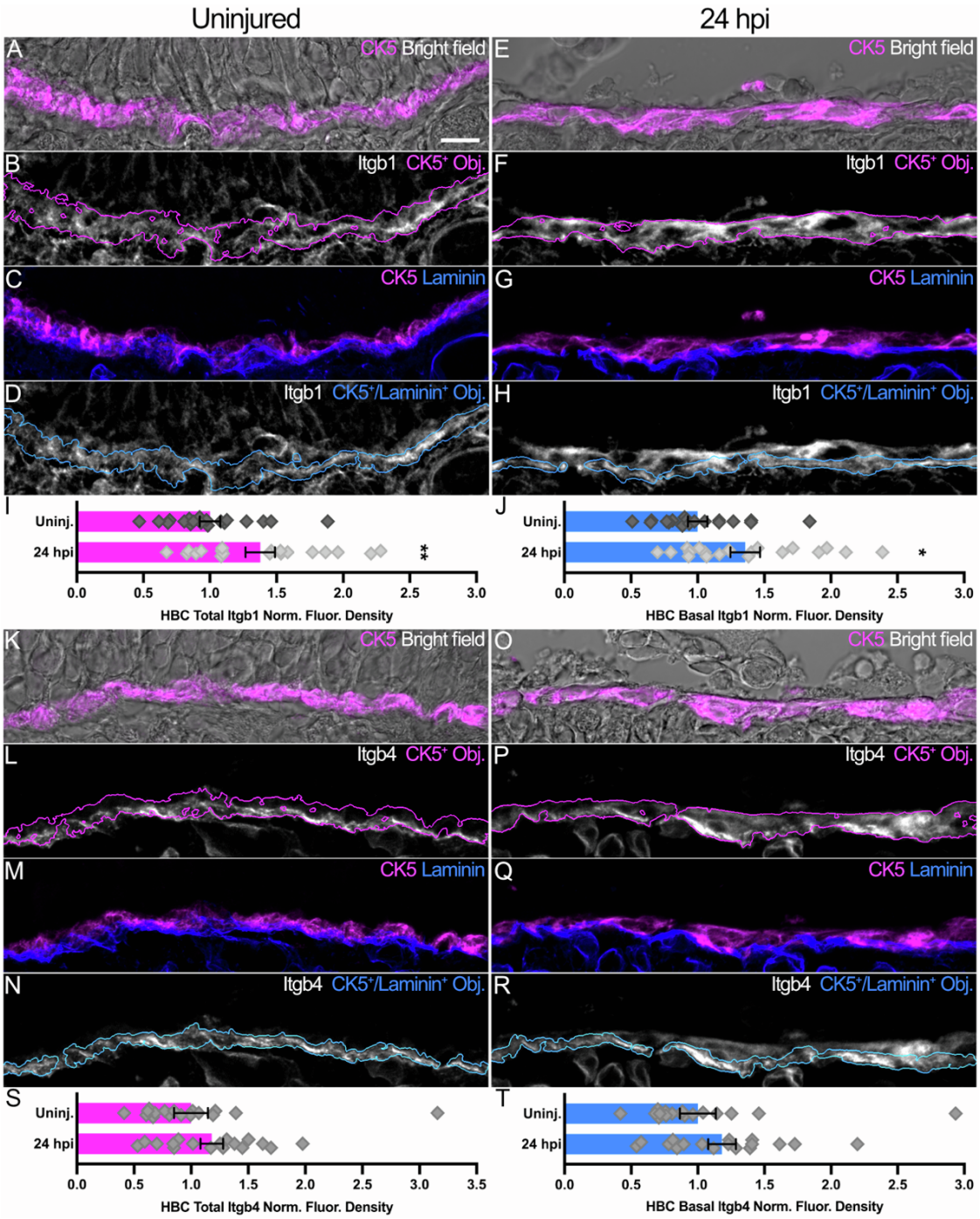

Figure S1: Despite p63 downregulation, HBCs at 24 hpi do not downregulate Itgb1 and Itgb4 (related to Figure 1). A-J: Identical regions illustrated in Figure 1F (A) and 1J (E) delineating total HBC area (magenta outlines in B and F). Identical regions illustrated in Figure 1G (C) and 1K (G) delineating HBC basal domains (blue outlines in D and H). Relative to HBCs within uninjured (uninj.) OE, HBCs at 24 hpi upregulate both total (I) and basal Itgb1 (J) (n = 3 mice across 19 regions). K-T: Identical regions illustrated in Figure 1O (K) and Figure 1S (O) delineating total HBC area (magenta outlines in L and P). Identical regions illustrated in Figure 1P (M) and 1T (Q) delineating HBC basal domains (blue outlines in N and R). Relative to HBCs within uninj. OE, HBCs at 24 hpi do not significantly alter their expression of both total (S) and basal Itgb4 (T) (n = 3 mice across 17 regions). Unpaired t-test (I, J), Mann-Whitney test (S, T). Uninj. used as baseline, error bars indicate mean ± SEM, *p<0.05, **p<0.01 (I, J, S, T). Scale bar equals 10 μm (A).

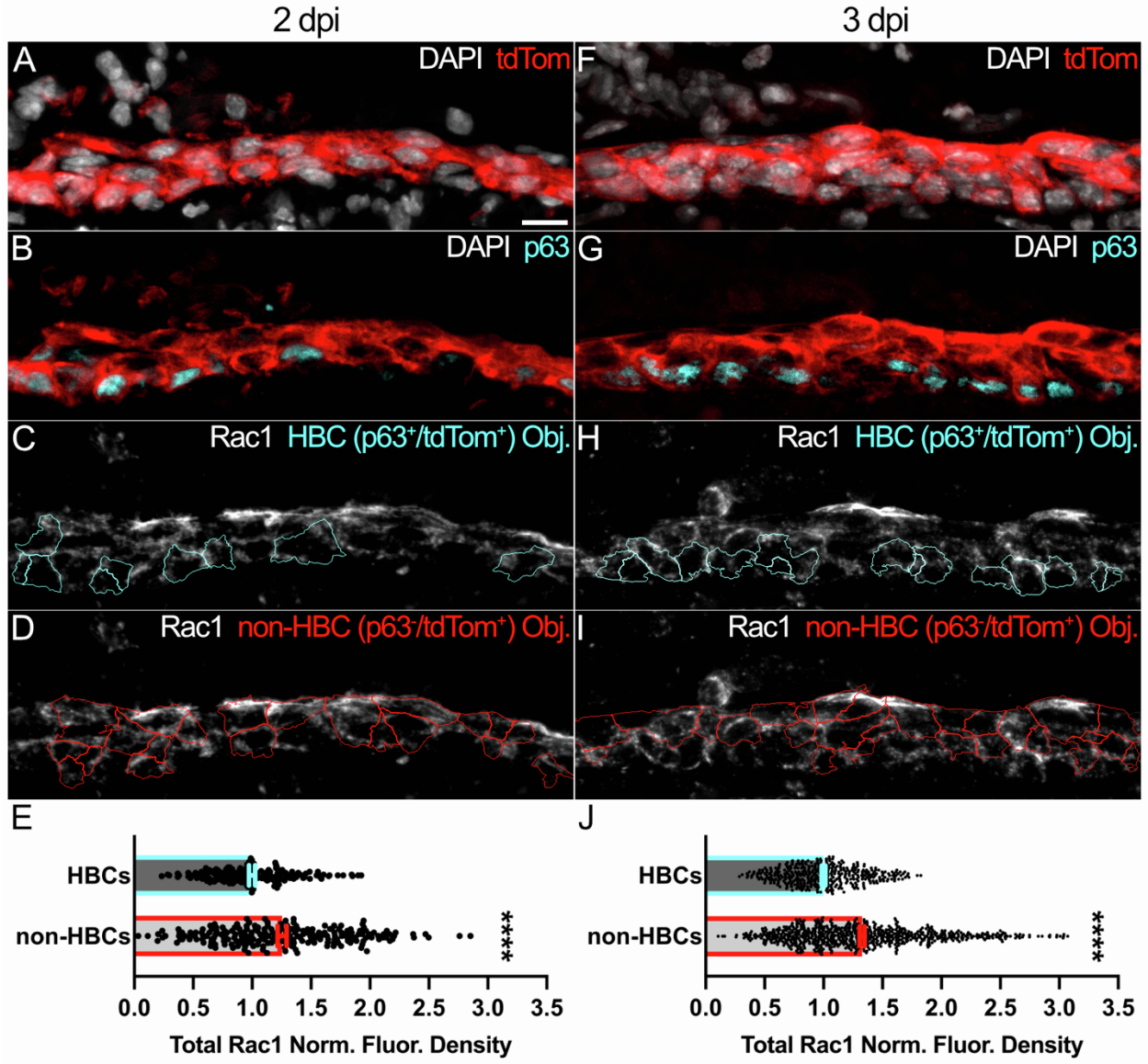

Figure S2: As OE regeneration proceeds, HBCs progressively diminish Rac1 expression relative to emerging non-HBCs (related to Figure 2). A-D: $p63^+/tdTom^+$ HBCs (cyan outlines in C) within the regenerating OE at 2 dpi (A, B) decrease Rac1 expression relative to $p63^-/tdTom^+$ non-HBCs (red outlines in D). E: Quantification of total Rac1 norm. fluor. density within $p63^+/tdTom^+$ HBCs and $p63^-/tdTom^+$ non-HBCs at 2 dpi, each point represents an analyzed obj. (as represented by cyan and red outlines, respectively, in C and D) (n = 3 mice, 176 $p63^-/tdTom^+$ HBCs and 218 $p63^-/tdTom^+$ non-HBCs). F-I: $p63^+/tdTom^+$ HBCs (cyan outlines in H) within the regenerating OE at 3 dpi (F, G) are at a further deficit in Rac1 expression relative to $p63^-/tdTom^+$ non-HBCs (red outlines in I). J: Quantification of total Rac1 norm. fluor. density within $p63^+/tdTom^+$ HBCs and $p63^-/tdTom^+$ non-HBCs at 3 dpi, each point represents an analyzed obj. (as represented by cyan and red outlines, respectively, in H and I) (n = 3 mice, 412 $p63^-/tdTom^+$ HBCs and 796 $p63^-/tdTom^+$ non-HBCs). Mann-Whitney test, $p63^+/tdTom^+$ HBCs used as baseline, error bars indicate mean ± SEM, ****$p<0.0001$ (E, J). Scale bar equals 10 μm (A).

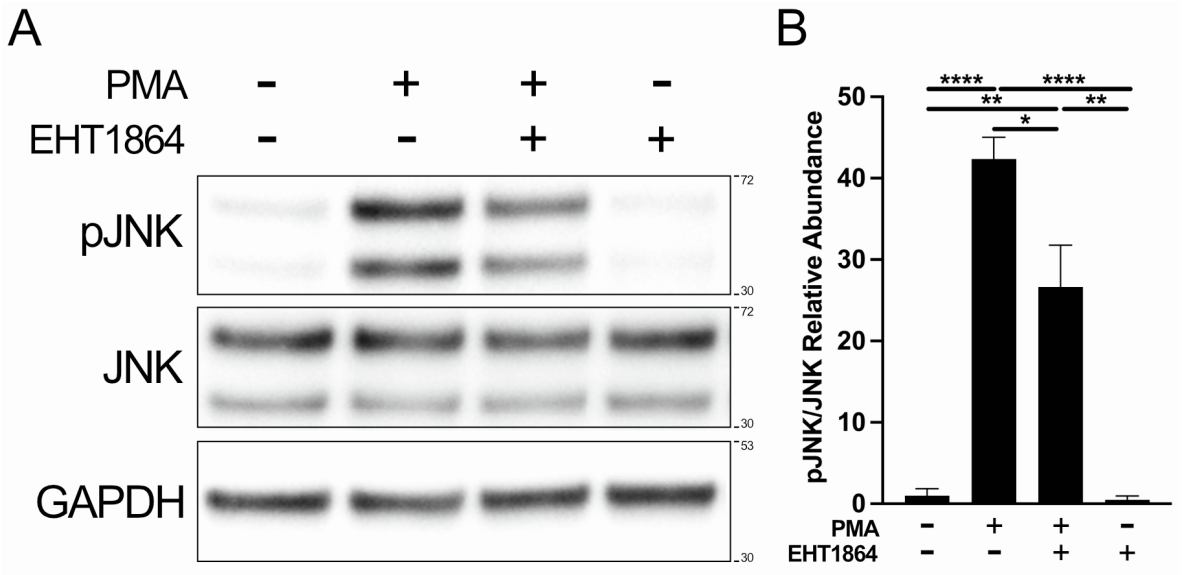

Figure S3: Primary HBCs activated *in vitro* enhance multiple components of Rac1-mediated signaling (related to Figure 3). A: Representative western blots depicting pJNK, total JNK, and GAPDH abundances in cultures of vehicle-treated (PMA-/EHT1864-), activated (PMA+/EHT1864-), activated and Rac1 inhibited (PMA+/EHT1864-), and Rac1 inhibited (PMA-/EHT1864+) HBCs. B: Quantification of densitometric measurements for normalized pJNK per normalized total JNK abundance (n = 3 independent trials), vehicle-treated used as baseline, error bars indicate mean + SEM, one-way ANOVA with post-hoc Tukey's multiple comparisons test, *<0.05, **p<0.01, ****p<0.0001.

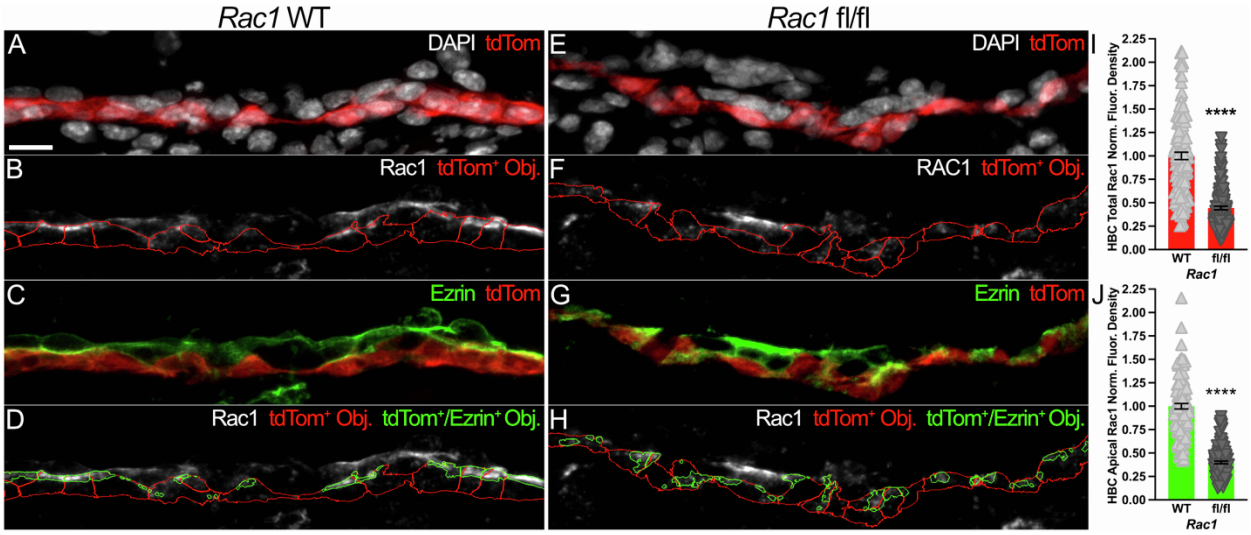

Figure S4: Decreased HBC-expressed total and apical Rac1 in *Rac1* fl/fl mice at 24 hpi (related to Figure 5). A-H: Representative immunofluorescence images demonstrating significantly decreased total (red outlines in B and F) and apical (green outlines in D and H) Rac1 expression within HBCs of *Rac1* fl/fl OE (E-H) relative to those found within *Rac1* WT OE (A-D). I: Quantification of total Rac1 norm. fluor. density within tdTom$^+$ HBCs, each triangle denotes an analyzed tdTom$^+$ Obj. as represented in B and F (n = 3 mice, 126 *Rac1* WT HBCs and 131 *Rac1* fl/fl HBCs). J: Quantification of Rac1 norm. fluor. density within tdTom$^+$ HBC apical domains, each triangle denotes an analyzed tdTom$^+$/Ezrin$^+$ Obj. as represented in D and H (n = 3 mice, 117 *Rac1* WT HBCs and 122 *Rac1* fl/fl HBCs). *Rac1* WT used as baseline, error bars indicate mean ± SEM, Mann-Whitney test, ****p<0.0001 (I, J). Scale bar equals 10 μm (A).

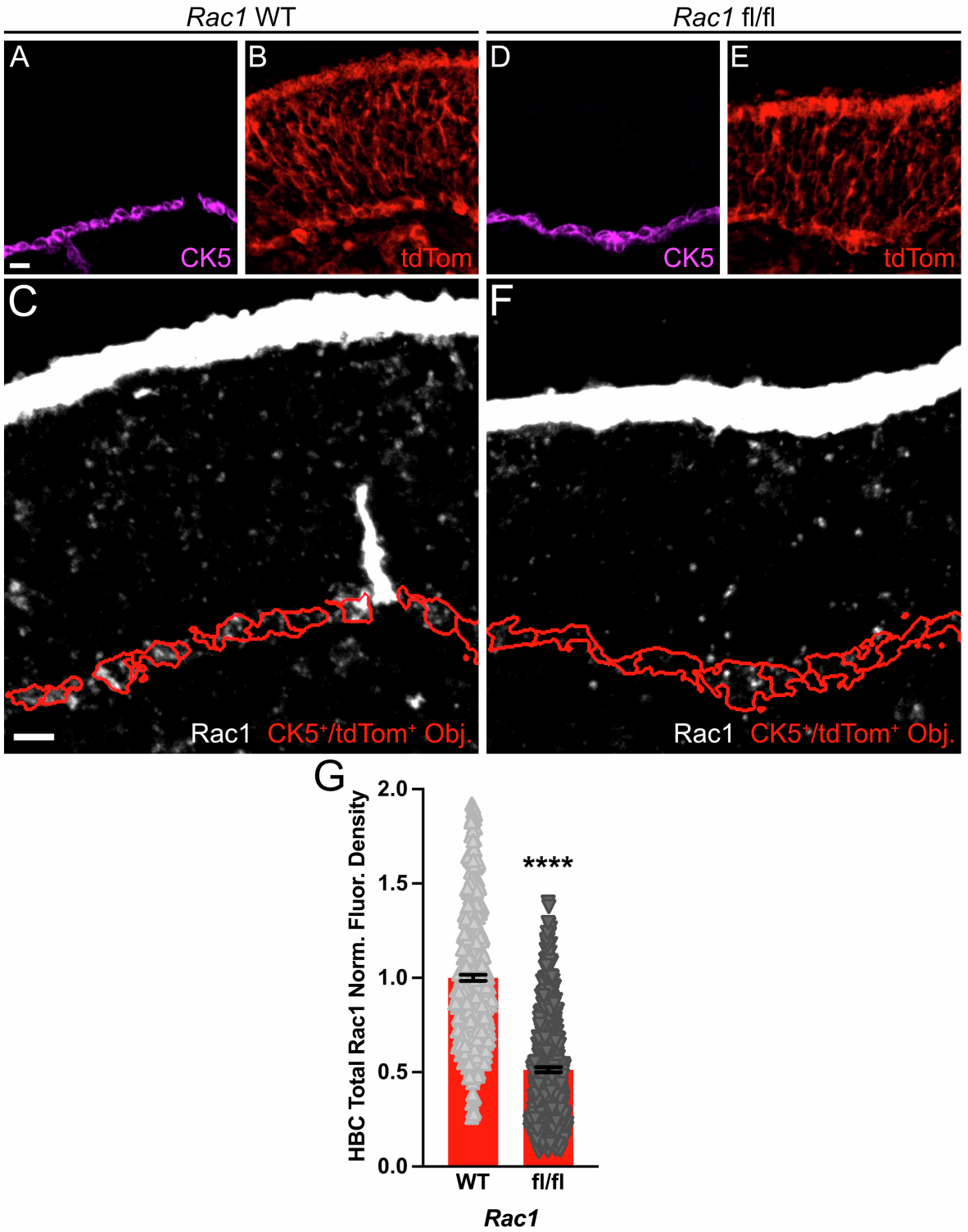

Figure S5: Decreased HBC-expressed Rac1 in *Rac1* fl/fl mice at 28 dpi (related to Figure 6). A-F: Immunofluorescence of Rac1 localized to CK5$^+$/tdTom$^+$ HBCs (within red outlines, C and F) at 28 dpi demonstrates persistent and decreased Rac1 expression in *Rac1* WT (A-C) and *Rac1* fl/fl (D-F) mice, respectively. G: Quantification of total Rac1 norm. fluor. density within CK5$^+$/tdTom$^+$ HBCs, each triangle denotes an analyzed CK5$^+$/tdTom$^+$ Obj. as represented in C and F (n = 3 mice, 436 *Rac1* WT HBCs and 477 *Rac1* fl/fl HBCs). *Rac1* WT used as baseline, error bars indicate mean ± SEM, Mann-Whitney test, ****p<0.0001 (G). Scale bar equals 10 μm (A, C).

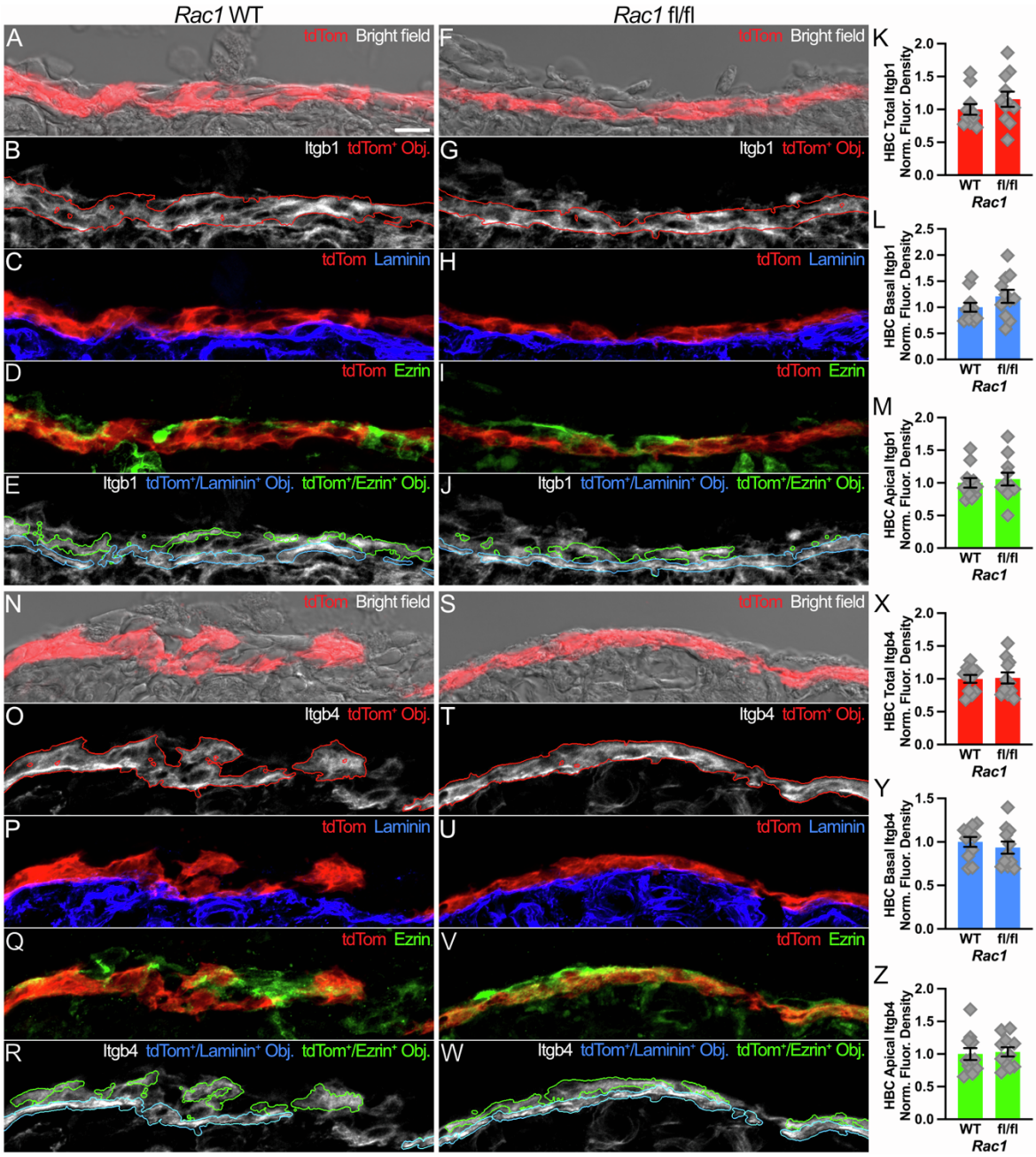

Figure S6: Itgb1 and Itgb4 expression within intracellular domains of tdTom$^+$ HBCs at 24 hpi is unaffected by HBC-specific *Rac1* cKO (related to Figure 5). A-J: Representative immunofluorescence images of tdTom$^+$ HBCs at 24 hpi (A, C, D, F, H, I) demonstrating that total (within red outlines, B and G), basal (within blue outlines, E and J), and apical (within green outlines, E and J) expression of Itgb1 is not significantly different between *Rac1* WT (A-E) and *Rac1* fl/fl (F-J) OE. K-M: Quantification of total (K), basal (L), and apical (M) Itgb1 norm. fluor. density within tdTom$^+$ HBCs, each diamond denotes an analyzed region as represented in B and G (K) and E and J (L and M) (n = 11 regions across 3 mice). N-W: Representative immunofluorescence images of tdTom$^+$ HBCs at 24 hpi (N, P, Q, S, U, V) demonstrating that total (within red outlines, O and T), basal (within blue outlines, R and W), and apical (within green outlines, R and W) expression of Itgb4 is not significantly different between *Rac1* WT (N-R) and *Rac1* fl/fl (S-W) OE. X-Z: Quantification of total (X), basal (Y), and apical (Z) Itgb4 norm. fluor. density within tdTom$^+$ HBCs, each diamond denotes an analyzed region as represented in O and T (X) and R and W (Y and Z) (n = 11 regions across 3 mice). Mann-Whitney test (K, L), unpaired t-test (M, X-Z). *Rac1* WT used as baseline, error bars indicate mean ± SEM. Scale bar equals 10 μm (A).

Table S1: Antibodies used for immunofluorescent labeling and their associated conditions (related to STAR Methods).

Antibody	Source	Identifier	Dilution	Antigen Retrieval Required	Signal Detection
Mouse α-p63	ATCC	Clone 4A4	1:100	Yes	Secondary fluorophore
Mouse α-Ezrin	Developmental Studies Hybridoma Bank	CPTC-Ezrin-1	1:25	No	SA-fluorophore
Rabbit α-Laminin	Novus Biologicals	NB300-144	1:100	No	Secondary fluorophore
Goat α-Itgb1	R&D Systems	AF2405	1:13	No	Secondary fluorophore
Rat α-Itgb4	R&D Systems	MAB4054	1:20	No	Secondary fluorophore
Chicken α-CK5	BioLegend	Clone Poly9059	1:200	No	Secondary fluorophore
Rabbit α-Rac1	Proteintech	24072-1-AP	1:200	Yes	TSA
Rabbit α-pFAKY925	Cell Signaling Technology	3284	1:100	Yes	TSA
Rabbit α-pcJun	Cell Signaling Technology	3270	1:40	Yes	TSA
Rabbit α-PGP9.5	Proteintech	14730-1-AP	1:200	Yes	Secondary fluorophore